

High-Temperature Hall Effect in $\text{Ga}_{1-x}\text{Mn}_x\text{As}$

D. Ruzmetov,¹ J. Scherschligt,¹ David V. Baxter,^{1,*} T. Wojtowicz,^{2,3}
X. Liu,² Y. Sasaki,² J.K. Furdyna,² K.M. Yu,⁴ and W. Walukiewicz⁴

¹*Dept. of Physics, Indiana University, Bloomington, IN, 47405, USA*

²*Dept. of Physics, University of Notre Dame, Notre Dame, IN, 46556, USA*

³*Institute of Physics, Polish Academy of Science, aleja Lotnikow 32/46, 02-668, Warsaw, Poland*

⁴*Materials Sciences Division, Lawrence Berkeley National Laboratory, Berkeley, CA, 94720, USA*

(Dated: December 30, 2021)

The temperature dependence of the Hall coefficient of a series of ferromagnetic $\text{Ga}_{1-x}\text{Mn}_x\text{As}$ samples is measured in the temperature range $80\text{ K} < T < 500\text{ K}$. We model the Hall coefficient assuming a magnetic susceptibility given by the Curie-Weiss law, a spontaneous Hall coefficient proportional to $\rho_{xx}^2(T)$, and including a constant diamagnetic contribution in the susceptibility. For all low resistivity samples this model provides excellent fits to the measured data up to $T=380\text{ K}$ and allows extraction of the hole concentration (p). The calculated p are compared to alternative methods of determining hole densities in these materials: pulsed high magnetic field (up to 55 Tesla) technique at low temperatures (less than the Curie temperature), and electrochemical capacitance-voltage profiling. We find that the Anomalous Hall Effect (AHE) contribution to ρ_{xy} is substantial even well above the Curie temperature. Measurements of the Hall effect in this temperature regime can be used as a testing ground for theoretical descriptions of transport in these materials. We find that our data are consistent with recently published theories of the AHE, but they are inconsistent with theoretical models previously used to describe the AHE in conventional magnetic materials.

I. INTRODUCTION

Random alloys of GaAs and Mn have attracted interest from a number of research groups^{1,2,3,4}. Over a limited composition range $\text{Ga}_{1-x}\text{Mn}_x\text{As}$ is ferromagnetic with a Curie temperature as high as 140 K ¹ and Mn content x up to 0.1. This class of III-V diluted magnetic semiconductors (DMS) are fabricated by means of low temperature molecular beam epitaxy (MBE) which insures that most of Mn atoms randomly substitute cations in their crystal positions. They are promising materials in spintronics due to their potential for tuning their ferromagnetic and electric properties by means of electrical field⁵, optical excitation⁶, or impurities⁷. Ferromagnetic GaMnAs can be grown isomorphically within semiconductor structures and may be suitable for spin injection into GaAs based devices².

A complete theory of ferromagnetism in GaMnAs has yet to be established, but there is general agreement that a ferromagnetic coupling between local moments on the Mn ions is mediated by holes moving through the lattice. A variety of different theoretical frameworks have been put forward, ranging from a mean-field approach with essentially free carriers^{3,4} to approaches that assume the carrier dynamics to be dominated by the proximity of the system to the metal insulator transition⁸ and the importance of disorder on the magnetic state⁹. To date many of the claims regarding the relevance of these theories have been based upon their ability to predict the ferromagnetic transition temperature. In trying to distinguish between these many competing theories it is essential to explore as wide a range of physical properties as possible. Noting that these alloys span a wide range of conductivities, measurements of electronic transport could be particularly useful in this regard.

Since it is generally agreed that holes mediate the ferromagnetic interaction between Mn ions the hole concentration is a crucial parameter for determining the properties of these materials. It influences essentially all their major properties^{3,4}. Therefore it is also important to measure the carrier density and understand the physical factors that control it in order to improve our knowledge of these materials. However, the disorder in GaMnAs results in a carrier concentration (p) that is generally lower than the Mn density making an independent measurement of p necessary. Determination of the carrier density by means of the Hall effect is complicated due to the presence of the Anomalous Hall contribution arising from the broken symmetry provided by the magnetisation. A conventional way to solve this problem is going to low temperatures and high (above 20 Tesla) magnetic fields where the magnetization and magnetoresistance saturate making possible to extract the Ordinary Hall coefficient^{10,11}. Limited accessibility of this method has stimulated the search for other techniques of determining p ^{12,13}.

In this paper we measure the Hall effect in a series of $\text{Ga}_{1-x}\text{Mn}_x\text{As}$ samples at temperatures above T_c in order to provide insight on both of these fronts (testing our understanding and providing a means for measuring the carrier concentration). Our results provide support for the recent theory of Jungwirth *et al*^{14,15} suggesting that a clean-limit theory can successfully describe transport in these materials over a range of compositions. We also demonstrate that Hall measurements in this temperature range can be used to find the hole concentration without the need to resort to high magnetic fields. The temperature dependence of the Hall coefficient in this paramagnetic regime may be described by a model that accounts for the paramagnetic contribution to the Anomalous Hall Effect (AHE) together with the Ordinary Hall

Effect (OHE). With this model we demonstrate that the AHE can dominate the Hall resistivity in GaMnAs even above room temperature. However, by properly accounting for this contribution the carrier concentration can be determined from the measurements.

II. EXPERIMENT

GaMnAs films were grown by means of MBE at a substrate temperature $T_s = 275^\circ\text{C}$. The sample structures were as follows: semi-insulating GaAs (100) substrate/100 nm of GaAs deposited by MBE at $T_s = 590^\circ\text{C}$ /30–100 nm of GaAs deposited by MBE at $T_s = 275^\circ\text{C}$ /GaMnAs film with thicknesses of 123 nm or 300 nm. All films demonstrate an in-plane easy axis of the magnetization. The samples were patterned for transport measurements in a standard Hall-bar geometry with dimensions between the longitudinal voltage contacts of $0.9 \times 0.3 \text{ mm}^2$. For High-Temperature Hall and resistivity measurements we used an MMR Technologies R2105-26 Thermal Stage System employing Joule-Thomson Effect to vary sample temperatures in the range 80–500 K. The samples were mounted on the thermal stage with silicon grease and were kept in $\sim 15 \text{ mTorr}$ vacuum during measurements. The thermal stage was placed between the poles of an electromagnet so that a DC magnetic field (up to 5 kOe) could be directed perpendicular to the sample plane. The samples were wired with golden wires and soldered with Indium. The contacts worked even above the In melting point (430 K) since the wires were held on the sample by surface tension of liquid In.

Transport measurements above 80 K were done using standard Lock-in techniques with excitation current of $100 \mu\text{A}$ and frequency 17 Hz and also some of the results were confirmed with DC measurements using Keithley current source 220 and nano-voltmeter 182. Each Hall coefficient data point was obtained from the slope of a straight line fitted to at least 6 data points of the Hall resistance vs. field curve for a magnetic field ranging from -5 kOe to $+5 \text{ kOe}$. We also did some measurements in van der Pauw geometry which agreed with Hall-bar measurements. The low temperature (below 80 K) transport measurements were performed in a liquid He cryostat using Quantum Design digital bridge model 1802 with $50 \mu\text{A}$ excitation current. The Hall coefficients below the Curie temperature were measured at such magnetic fields that the sample magnetization in the growth (hard) direction was well below the saturation, which typically corresponded to a range $-500 \text{ Oe} < H < +500 \text{ Oe}$. The magnetization of ferromagnetic GaMnAs was measured in a Quantum Design MPMS XL Superconducting Quantum Interference Device magnetometer. Annealing of GaMnAs samples was done in situ on the MMR thermal stage between transport measurements. The sample was heated to 260°C and kept for 2 hrs in 15 mTorr vacuum. Similar samples annealed on a specially designed annealing apparatus in a high purity Ar gas mass-controlled

flow and with short ($\sim 5 \text{ min}$) heating up and cooling down times showed the same magnetic and transport properties as the ones annealed on the MMR stage.

III. RESULTS AND DISCUSSION

The bulk resistivity and the Hall coefficient:

$$R_{Hall} \equiv \frac{\rho_{xy}}{H_z} = \frac{E_y}{j_x H_z} \quad (1)$$

where ρ_{xy} is the Hall resistivity, E and H are electric and magnetic fields, and j is current density, were measured in a wide temperature range 2 – 420 K using a conventional LHe cryostat below 100 K and the MMR thermal stage above 80 K. The temperature dependence of R_{Hall} and the resistivity for a representative sample with $x = 0.048$ are shown in Fig. 1. The Hall coefficient and resistivity exhibit maxima approximately at the Curie temperature (T_c) 53 K. Note that the Hall coefficient continues to change with T above 300 K, which is an indication of the presence of the temperature dependent anomalous Hall effect.

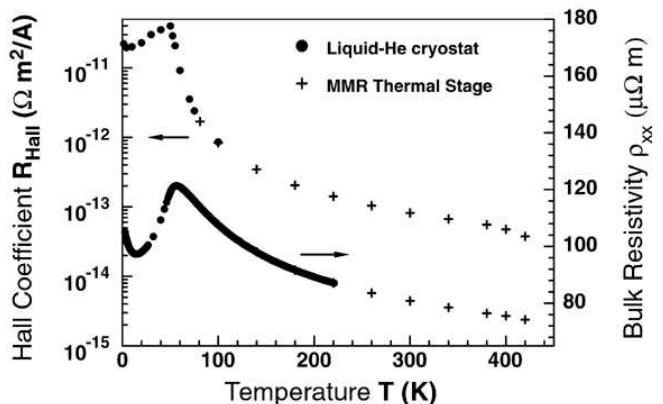


FIG. 1: Hall coefficient and resistivity of GaMnAs ($x = 0.048$, $T_c = 53 \text{ K}$) were measured in a wide temperature range using Liq-He cryostat below 100 K and MMR Joule-Thomson refrigerator above 80 K. The Hall measurements were made over a field range of $\pm 5 \text{ kOe}$ for temperatures above T_c (on the MMR system) and over a range of $\pm 500 \text{ Oe}$ below T_c (in the Liq-He cryostat).

To account for the measured R_{Hall} temperature dependence we modeled the Hall effect as a sum of the Ordinary (OHE) and Anomalous¹⁶ (AHE) Hall contributions:

$$R_{Hall} = \frac{\mu_o}{e \cdot p} + R_s \cdot \left(-\frac{\chi_c}{T - \theta} + \chi_o \right) \quad (2)$$

The first term in Eq. (2) is the ordinary Hall coefficient due to the Lorentz force with μ_o being magnetic permeability of the vacuum, e – the magnitude of the electron charge, and p standing for the free hole concentration. The AHE is proportional to the magnetization of the

sample and this takes the form of the second term in the equation in the paramagnetic regime. $R_s = \gamma_{para} \cdot \rho_{xx}^n(T)$ is the spontaneous Hall coefficient with γ_{para} and n – temperature independent parameters, and ρ_{xx} – the bulk resistivity of the GaMnAs film. We model the paramagnetic susceptibility following Curie-Weiss law with $\chi_c = \mu_o N_{Mn} g^2 J(J+1) \mu_B^2 / (3k_B)$ – the Curie constant taking $g = 2$ and $J = 5/2$, and θ is the Curie-Weiss temperature. χ_o is a temperature independent correction to the paramagnetic susceptibility which is necessary to be included in order to adequately describe the measured data with a single form for R_s . χ_o is the same for all samples and always smaller than the paramagnetic term in our fits.

We were able to fit this model with $n = 2$ to the measured data for all samples with room temperature resistivities less than $100 \mu\Omega\text{m}$. Carrier concentrations were extracted from these fits. A typical fit is shown in Fig. 2 along with the separate contributions from the OHE and AHE. In order to show the influence of the χ_o cor-

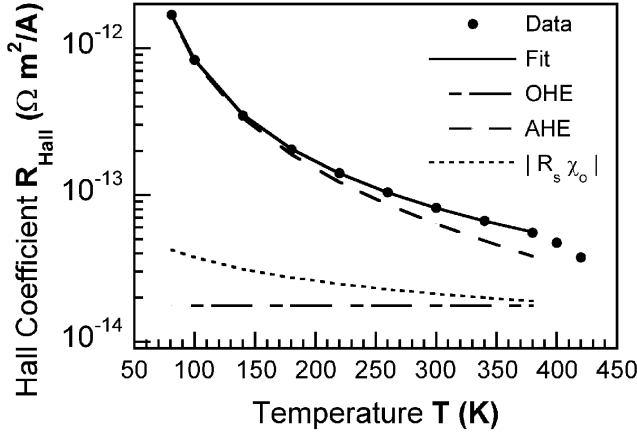


FIG. 2: Fitting to the measured Hall coefficient of the $x = 0.048$ sample with $T_c = 53$ K. Fit is Eq. (2) and is the sum of AHE and OHE. Fitting parameters: $p = 4.5 \times 10^{-20} \text{ cm}^{-3}$, $\gamma_{para} = 0.033 (\text{A} \cdot \Omega)^{-1}$, $\theta = 57$ K, $\chi_o = -10^{-4}$. The dotted line shows the absolute value of the contribution to the R_{Hall} due to χ_o . Note that although χ_o is itself a constant, the corresponding contribution to the Hall coefficient varies with temperature due to the dependence of R_s (in Eq. 2) on the longitudinal resistivity.

rection the figure includes the $|R_s \cdot \chi_o|$ term. One can see that our model perfectly fits the data up to 380 K. For this sample the AHE contribution dominates over OHE in the whole temperature range of the fit. The fitted Curie-Weiss temperature is slightly bigger than T_c which is a common thing in ferromagnetic metals¹⁷. Since χ_o was held constant for all samples, p , θ , and γ_{para} were essentially the only free parameters in the fit for each sample. The Curie-Weiss temperature θ was allowed to vary but the optimal value was always within 4 K of T_c determined from SQUID magnetometer measurements. To

confirm the reliability of our method we estimate γ_{para} from independent measurements of the AHE at 4.2 K using the relation $\rho_{xy} = \gamma_{ferro} \cdot \rho_{xx}^2 M$, since at this temperature an independent measurement of M is possible. Hall (ρ_{xy}) and bulk ($\rho_{xx} = 103 \pm 2 \mu\Omega\text{m}$) resistivities were measured in the LHe cryostat at 4.2 K (Fig. 3a) and magnetization M was found in the MPMS (Fig. 3b). The magnetic field was in the hard axis direction which

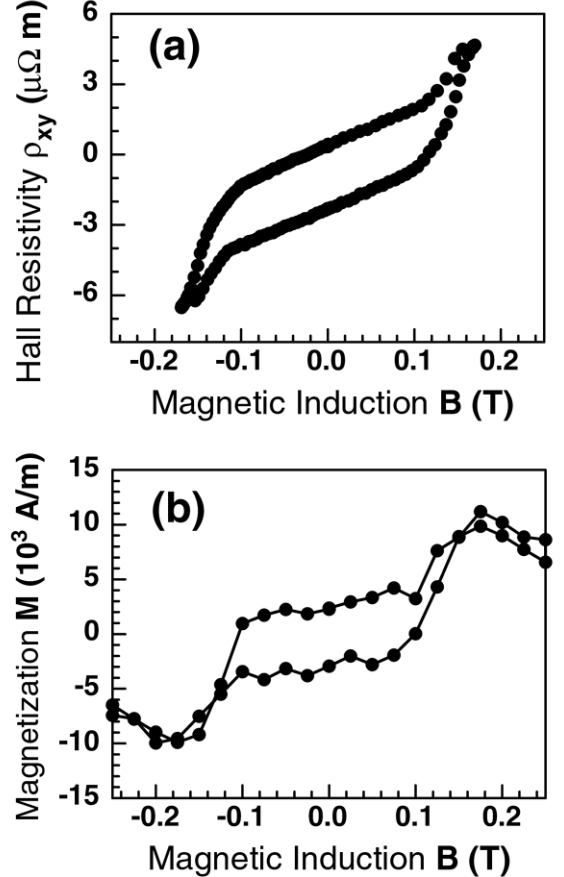


FIG. 3: Measured Hall resistivity (a) and magnetization (b) of $\text{Ga}_{1-x}\text{Mn}_x\text{As}$ $x = 0.048$ sample at 4.2 K. Magnetic field is in the hard axis direction. The magnetization graph shows raw SQUID data (circles) which includes diamagnetic contribution from the GaAs substrate.

explains relatively large coercive force of ~ 0.12 T and small magnitude of the magnetization. In the MPMS data, the diamagnetic contribution from the GaAs substrate causes the magnitude of the measured magnetization to decrease above 0.18 T where the ferromagnetic signal saturates. But this does not affect our measurement of γ_{ferro} since the remnant magnetization and the Hall resistivity at $B = 0$ are used in the calculation. The value so obtained, $\gamma_{ferro} = 0.04 \pm 0.01 (\text{A}\Omega)^{-1}$, agrees within the uncertainties with γ_{para} determined from the fit $\gamma_{para} = 0.033 \pm 0.002 (\text{A}\Omega)^{-1}$ in the paramagnetic region. This result supports our model and is evidence that the relation $R_s = \gamma \cdot \rho_{xx}^2(T)$ is valid in a wide tempera-

TABLE I: Comparison of different methods of measuring the hole density for a set of $\text{Ga}_{1-x}\text{Mn}_x\text{As}$ samples. Calculation of p using: 1) R_{Hall} at 340 K assuming that the whole Hall voltage is due to the OHE, p_0 ; 2) high fields (above 25 T) and low temperatures at the Los Alamos National Lab facilities, p_1 (taken from ref. [11]); 3) electro-chemical capacitance voltage profiling at the Lawrence Berkeley National Lab, p_2 ; 4) the high-temperature Hall method described in this paper, p_3 .

x	Thick- ness (nm)	T_c (K)	$\rho_{xx}(300\text{ K})$ $\pm 5\%$ ($\mu\Omega\text{m}$)	γ_{para} ± 0.002 ($\text{A}\Omega$) $^{-1}$	p_0 ignoring AHE at 340K ($\times 10^{20}\text{ cm}^{-3}$)	p_1 [11] $T \ll T_c, H > 25\text{ T}$ ($\times 10^{20}\text{ cm}^{-3}$)	p_2 ECV ($\times 10^{20}\text{ cm}^{-3}$)	p_3 $T_c < T < 380\text{ K}$ ($\times 10^{20}\text{ cm}^{-3}$)
0.033	300	41	77	0.039	1.4 ± 0.1	3.7 ± 0.7	2.8 ± 0.6	2.8 ± 0.3
0.048	300	53	81	0.033	1.2 ± 0.1	3.0 ± 0.6	4.4 ± 0.3	4.5 ± 0.7
0.050	300	55	60	0.044	1.4 ± 0.1	4.5 ± 0.9	3.2 ± 0.6	4.4 ± 0.8
0.053	300	55	92	0.026	1.0 ± 0.1	2.3 ± 0.5	3.5 ± 0.3	4.0 ± 0.7
0.055	300	59	69	0.041	1.1 ± 0.1	—	4.5 ± 0.6	4.2 ± 0.7
0.072	124	63	127	—	0.45 ± 0.06	—	4.0 ± 0.3	$3_{-1}^{+2}{}^a$
0.072	124	84 ^b	79	0.031	0.80 ± 0.06	—	6.8 ± 0.7	6 ± 2

^a $n = 1.4$ (ρ_{xx} exponent) only in this fit;

^bAnnealed at 260°C for 2 hrs.

ture range (below and above T_c). This confirms that the physical mechanism responsible for the AHE is the same for ferromagnetic and paramagnetic phases of GaMnAs.

The carrier concentrations determined by our method (p_3) are summarized in the Table I. In determining p_3 , the spontaneous Hall coefficient for all low resistivity ($\rho_{xx}(300\text{ K}) < 100\mu\Omega\text{m}$) GaMnAs samples was assumed to vary as $R_s = \gamma_{para} \cdot \rho_{xx}^2(T)$. In the conventional treatment of the AHE¹⁶, a quadratic dependence of the Hall coefficient on the diagonal resistivity is taken to suggest that the side-jump is the dominant scattering mechanism in the studied material. However, since in this conventional picture the side jump mechanism causes the variation $\rho_{xy} \propto \rho_{xx}^2$ and the skew scattering varies as $\rho_{xy} \propto \rho_{xx}$, then one could expect $n = 2$ (exponent of ρ_{xx}) to be favored in high-resistivity materials. This disagrees with our observations when we see that $n = 2$ assumption works for low-resistivity samples and breaks down for high-resistivity ones. A good illustration of this is the fitting results for the $x = 0.072$ sample shown in Table I. The as grown sample with $x = 0.072$ has $\rho_{xx}(300\text{ K}) = 127\mu\Omega\text{m}$ and in this case it was necessary to set the exponent $n = 1.4$ (defined by $R_s = \gamma_{para} \cdot \rho_{xx}^n$) in order to achieve good fitting with Eq. (2). The room temperature resistivity of this sample decreases to $79\mu\Omega\text{m}$ upon annealing and a good fit with $n = 2$ becomes possible for this annealed sample. In general, samples with room temperature resistivity higher than $100\mu\Omega\text{m}$ show more rapid decrease of resistivity with increasing T and their Hall data cannot be fitted with $n = 2$. Samples with ρ_{xx} higher than $180\mu\Omega\text{m}$ cannot be fitted with any n . These highly resistive samples have large Mn concentrations (above 7%) and may lie on the insulator side of the metal-insulator transition¹⁸. It is worthwhile to note that the determination of p by means of the Hall effect measurements at high fields and

low temperatures also fails for insulating samples due to their large magnetoresistance¹⁸. We see that this limitation extends to the high-temperature technique as well.

On the other hand, the recent theory of the AHE in ferromagnetic semiconductors proposed by Jungwirth *et al*^{14,15} assumes that AHE arises as an anomalous contribution to the Hall conductivity σ_{xy} which in the absence of disorder in the material does not depend on ρ_{xx} . That should result in a Hall resistivity that is proportional to the second power of ρ_{xx} (from $\sigma_{xy} = -\rho_{xy}/(\rho_{xx}^2 + \rho_{xy}^2)$ using $\rho_{xy}^2 \ll \rho_{xx}^2$), i.e. the theory predicts $n = 2$ for clean samples. Then our fitting results show that the low resistivity samples, or equivalently the samples with low Mn concentration ($x < 0.06$), have the amount of defects low enough so that the Hall conductivity is not significantly affected by scattering and the GaMnAs crystal can be considered to be clean from the electron transport point of view (or at least regarding σ_{xy}). This explains why $n = 2$ law in Eq. (2) works for $\text{Ga}_{1-x}\text{Mn}_x\text{As}$ with $x < 0.06$. The samples with high Mn content and high resistivities have more defects in the lattice, so that the Hall conductivity is no longer defect (and ρ_{xx}) independent and the relation $\rho_{xy} \propto \rho_{xx}^2$ is no longer valid. Thus our ability to fit with $n = 2$ only the data from low resistivity samples is more consistent with this theoretical framework^{14,15} than it is with the conventional framework developed for metallic samples¹⁶.

In our fits, χ_o was taken to be -10^{-4} (dimensionless in SI units) for all samples. The fact that this parameter does not depend on temperature and Mn content suggests that it is due to the diamagnetic contribution of GaAs matrix, but its size is considerably larger than expected ($\chi_{GaAs} = -1.22 \times 10^{-6}$). This could reflect a difference between the efficiency of paramagnetic spins and diamagnetic currents in contributing to the anomalous Hall conductivity. If we modify Eq. (2) slightly by

writing $\chi_o = \nu\chi_{\text{GaAs}}$ where ν is the ratio $\gamma_{\text{diam}}/\gamma_{\text{para}}$, we find that $\gamma_{\text{diam}} = 82\gamma_{\text{para}}$. Alternatively, it is also possible that the parameterization we have used covers some other deviation from the Curie law in the paramagnetic susceptibility. Further work will be needed to resolve this.

Carrier concentrations of our samples were estimated using other techniques as well, as displayed in Table I. For four samples, the Hall resistance was measured at high magnetic field (up to 55 T in a pulse) and low temperature (down to 600 mK), where magnetization and magnetoresistance saturate and the slope of the Hall resistance is due only to the OHE¹¹. Such measurements were performed at Los Alamos National Lab and the results are shown in the Table I as p_1 . Table I also presents results of the hole concentration measurements by means of electrochemical capacitance-voltage (ECV) profiling, p_2 . The ECV method is described elsewhere¹⁹ but for now we note that it involves etching the sample which, therefore, is sacrificed during the measurement. The ECV profiling measurements showed little change of the hole concentration along the growth direction of the GaMnAs films, thus confirming that p was a single-defined quantity in our samples. One can see that hole densities measured by the present method (p_3) are within a factor of 2 of the high-field data (p_1) and within the uncertainties of ECV measurements (p_2). This shows that our method gives reasonable values of p while being relatively simple and non-destructive. Samples with high manganese concentration have bigger AHE contributions. This complicates the extraction of the OHE component and accounts for the large uncertainties for the sample with $x = 0.072$. Finally, to emphasize the importance of the AHE even at high temperatures, Table I also includes carrier concentrations obtained if you ignore AHE at 340 K, p_0 . These values are systematically lower than any of the other independent measurements of p . Therefore, as suggested in Fig. 2 for one sample, the AHE is significant even above room temperature in all the samples we measured and cannot be neglected in calculating the carrier densities.

An interesting feature of GaMnAs semiconductors is that their magnetic properties may be improved using low temperature annealing^{20,21,22}. We have measured the effect of annealing on the temperature dependence of the Hall and bulk resistivities for three samples with x equal 0.072, 0.085, and 0.087 which show an increase of the Curie temperature of 21 K, 25 K, and 26 K correspondingly upon annealing at 260°C for 2 hrs. The measured data and their fits for $x = 0.072$ are shown in Fig. 4. These samples with high Mn concentration have large resistivities (up to $632\mu\Omega\text{m}$ at 300 K for as grown $x = 0.085$) and their Hall coefficients at 300 K are roughly 5 times bigger than for the samples with $x \leq 0.055$. For all measured samples, the bulk resistivity and Hall coefficient decrease upon annealing (except at the temperatures close to T_c where Curie-Weiss susceptibility diverges). Fitting to the measured data for

$x = 0.072$ reveals an approximately 100% increase of the carrier concentration due to annealing, which naturally contributes to the decrease of the bulk resistivity.

At temperatures above 350–400 K all studied samples show a simultaneous drop in the Hall coefficient and bulk resistivity. At sufficiently high temperatures the Hall coefficient changes sign and increases rapidly in magnitude. The effect is reproducible for different temperature scans. An example for $x = 0.072$ is displayed in the Fig. 5. The samples with lower Mn concentration (3–5%) exhibit the drop at higher temperature, which looks qualitatively the same as in Fig. 5 but is shifted ~ 50 K to the right. This feature limited the fitting range of our calculations below 380 K (below 340 K for the sample in Fig. 5). In order to check the possibility of a thermally activated parallel conductance through the material underneath the GaMnAs film, we measured the bulk resistance of a bare GaAs substrate and Low-T MBE-deposited GaAs film on a GaAs substrate used as a buffer layer for GaMnAs. The resistances found at 400 K are 4 orders of magnitude bigger than the resistances of GaMnAs films which makes unlikely the possibility of the parallel conductance through the bulk GaAs. However, the conductance may be due to an inversion layer formed at the interface between GaMnAs film and GaAs buffer. A similar effect of the resistivity drop and the sign change of the magnetoresistance at high temperatures was observed and studied for thin films on Si substrates and explained by the formation of the inversion layer on the film/Si interface^{23,24}. This phenomenon may limit the utility of our technique for samples with higher T_c 's which would require extending the fitting range to higher temperatures where the parallel conductance through an inversion layer or substrate becomes appreciable.

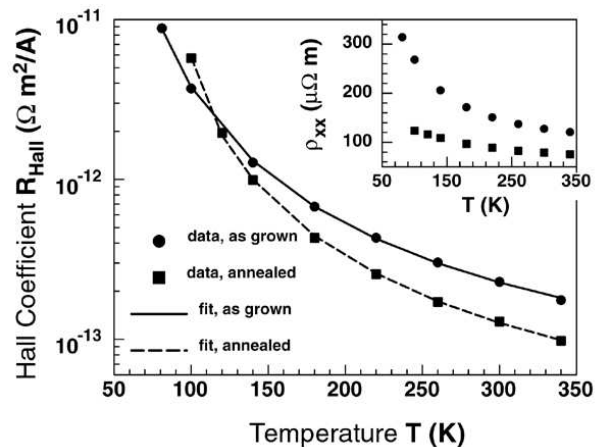


FIG. 4: Annealing effect on the Hall coefficient and bulk resistivity for $x = 0.072$. The T_c raises from 63 K to 84 K upon annealing at 262°C for 2 hrs.

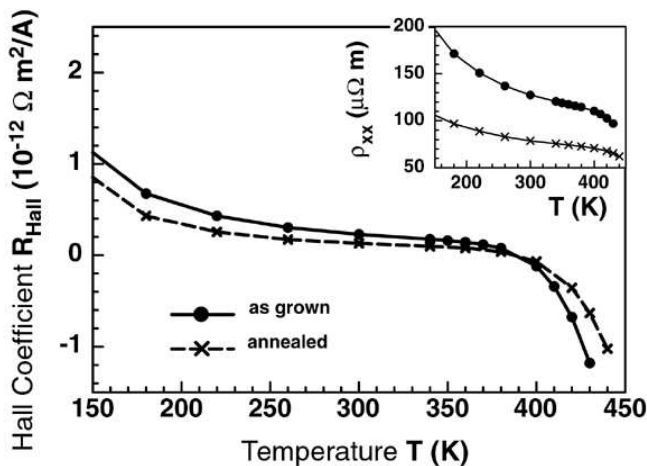


FIG. 5: High temperature behavior of the Hall coefficient and bulk resistivity for $x = 0.072$. Symbols are measured data, lines are guides for an eye.

IV. CONCLUSIONS

The results of the Hall effect measurements of a series of GaMnAs samples above the Curie temperature and up to 380 K can be described with a model equation which takes into account the ordinary and anomalous contributions to the Hall resistivity. The good agreement between the measured and fitting Hall data suggests that the model correctly captures the physical origin of the Hall effect above T_c and up to 380 K. We found that the anomalous contribution to the Hall resistivity dominates over ordinary contribution up to 380 K in all samples. The fitting procedure based on our model can be used as a new technique to determine the hole concentrations in GaMnAs, which are notoriously difficult to measure by conventional methods. The hole densities determined by our method agree with independent measurements of carrier concentrations in our GaMnAs samples done by

means of ECV profiling.

The results of the analysis of the measured data based on our model allow to discriminate between different existing theoretical approaches to the anomalous Hall effect. Particularly, our observations of the AHE are more consistent with a recently proposed theory of the Hall conductivity in GaMnAs by Jungwirth *et al.*^{14,15} than they are with conventional theory which ascribes the AHE to be due to the spin dependent scattering such as skew scattering or side jump¹⁶.

It is found that the temperature dependence of the anomalous Hall effect above T_c can be described with the Curie-Weiss law for the paramagnetic susceptibility with the inclusion of a small, negative, temperature and Mn content independent correction to the susceptibility. The origin of this correction is not clear. It may be due to the diamagnetic contribution from the GaAs matrix, but demonstrating this will require an explanation for its anomalous size compared to the paramagnetic contribution.

The Hall coefficient and bulk resistivity of all studied samples exhibit a drop above 400 K. The reason of such a dramatic change of the transport parameters at high temperatures is not understood yet but may be caused by parallel conductance through an inversion layer on the interface between the substrate and the GaMnAs film. This phenomenon complicates the study of the transport properties of these materials above 400 K.

Acknowledgments

The authors gratefully acknowledge discussions with A. C. Ehrlich, J. Kikkawa, A. H. MacDonald, and T. Jungwirth. This work was supported by the Office of Naval Research and the Research Foundation for the State University of New York under grant number N000140010951 and by the 21st Century Science and Technology Fund of the State of Indiana.

* E-mail address: baxterd@indiana.edu

¹ K. W. Edmonds, K. Y. Wang, R. P. Campion, A. C. Neumann, N. R. S. Farley, B. L. Gallagher, C. T. Foxon, Appl. Phys. Lett. **81**, 4991 (2002).

² Y. Ohno, D. K. Young, B. Beschoten, F. Matsukura, H. Ohno, D. D. Awschalom, Nature (London) **402**, 790 (1999).

³ T. Dietl, H. Ohno, F. Matsukura, Phys. Rev. B **63**, 195205 (2001); T. Dietl, H. Ohno, F. Matsukura, J. Cibert, D. Ferrand, Science **287**, 1019 (2000).

⁴ J. König, J. Schliemann, T. Jungwirth, A. H. MacDonald, cond-mat/0111314, in *Electronic Structure and Magnetism of Complex Materials*, ed. D. J. Singh and D. A. Papaconstantopoulos, (Springer-Verlag, 2002).

⁵ H. Ohno, D. Chiba, F. Matsukura, T. Omiya, E. Abe, T. Dietl, Y. Ohno, K. Ohtani, Nature (London) **408**, 944

(2000).

⁶ S. Koshihara, A. Oiwa, M. Hirasawa, S. Katsumoto, Y. Iye, C. Urano, H. Takagi, H. Muneoka, Phys. Rev. Lett. **78**, 4617 (1997).

⁷ Y. Satoh, D. Okazawa, A. Nagashima, J. Yoshino, Physica E **10**, 196 (2001).

⁸ M. Berciu, R. N. Bhatt, Phys. Rev. Lett. **87** 107203 (2001).

⁹ S. Das Sarma, E. H. Hwang, A. Kaminski, Phys. Rev. B **67** 155201 (2003).

¹⁰ T. Omiya, F. Matsukura, T. Dietl, Y. Ohno, T. Sakon, M. Motokawa, H. Ohno, Physica E **7**, 976 (2000).

¹¹ D. V. Baxter, D. Ruzmetov, J. Scherschligt, Y. Sasaki, X. Liu, J. K. Furdyna, C. H. Mielke, Phys. Rev. B **65**, 212407 (2002).

¹² K. M. Yu, W. Walukiewicz, T. Wojtowicz, W. L. Lim, X. Liu, Y. Sasaki, M. Dobrowolska, J. K. Furdyna, Appl.

- Phys. Lett. **81**, 844 (2002).
- ¹³ M. J. Seong, S. H. Chun, H. M. Cheong, N. Samarth, A. Mascarenhas, Phys. Rev. B **66**, 033202 (2002).
 - ¹⁴ T. Jungwirth, Q. Niu, A. H. MacDonald, Phys. Rev. Lett. **88**, 207208 (2002).
 - ¹⁵ T. Jungwirth, J. Sinova, K. Y. Wang, K. W. Edmonds, R. P. Campion, B. L. Gallagher, C. T. Foxon, Q. Niu, A. H. MacDonald, Appl. Phys. Lett. **83**, 320 (2003).
 - ¹⁶ *The Hall Effect and Its Applications*, edited by C. L. Chien and C. R. Westgate (Plenum, New York, 1980), pp. 43-51, 56-67.
 - ¹⁷ D. H. Martin, *Magnetism in Solids*, (The MIT press, Cambridge, Massachusetts, 1967), p. 20.
 - ¹⁸ H. Ohno, J. Magn. Magn. Mater. **200**, 110 (1999).
 - ¹⁹ M. M. Faktor, T. Ambridge, C. R. Elliott, J. C. Regnault in *Current Topics in Materials Science*, (North Holland, Amsterdam, 1980), Vol. 6, ed. E. Kaldis, pp. 1-107; P. Blood, Semicond. Sci. Technol. **1**, 7 (1986).
 - ²⁰ T. Hayashi, Y. Hashimoto, S. Katsumoto, Y. Iye, Appl. Phys. Lett. **78**, 1691 (2001).
 - ²¹ S. J. Potashnik, K. C. Ku, S. H. Chun, J. J. Berry, N. Samarth, P. Schiffer, Appl. Phys. Lett. **79**, 1495 (2001).
 - ²² K. M. Yu, W. Walukiewicz, T. Wojtowicz, I. Kuryliszyn, X. Liu, Y. Sasaki, J. K. Furdyna, Phys. Rev. B **65**, 201303(R) (2002).
 - ²³ J. K. Tang, J. B. Dai, K. Y. Wang, W. L. Zhou, N. Ruzyski, U. Diebold, J. Appl. Phys. **91**, 8411 (2002).
 - ²⁴ J. Dai, L. Spinu, K. Y. Wang, L. Malkinski, J. Tang, J. Phys. D **33**, L65 (2000).